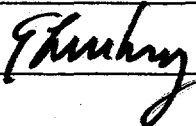


## U. S. DEPARTMENT OF ENERGY

UNIVERSITY CONTRACTOR, GRANTEE, AND COOPERATIVE AGREEMENT  
RECOMMENDATIONS FOR ANNOUNCEMENT AND DISTRIBUTION OF DOCUMENTS*See Instructions on Reverse Side*

1. DOE Report No. DOE/PC/91306-14	3. Title Sorption and Chemical Transformation of PAH's on Coal Fly Ash
2. DOE Contract No. DOE-DE-FG22-91PC91306	
4. Type of Document ("x" one) <input checked="" type="checkbox"/> a. Scientific and technical report <input type="checkbox"/> b. Conference paper: Title of conference _____	
Date of conference _____	
Exact location of conference _____	
Sponsoring organization _____	
<input type="checkbox"/> c. Other (Specify) _____	
5. Recommended Announcement and Distribution ("x" one) <input checked="" type="checkbox"/> a. Unrestricted unlimited distribution. <input type="checkbox"/> b. Make available only within DOE and to DOE contractors and other U. S. Government agencies and their contractors. <input type="checkbox"/> c. Other (Specify) _____	
6. Reason for Recommended Restrictions	
7. Patent and Copyright Information: Does this information product disclose any new equipment, process, or material? <input checked="" type="checkbox"/> No <input type="checkbox"/> Yes If so, identify page nos. _____ Has an invention disclosure been submitted to DOE covering any aspect of this information product? <input checked="" type="checkbox"/> No <input type="checkbox"/> Yes If so, identify the DOE (or other) disclosure number and to whom the disclosure was submitted. Are there any patent-related objections to the release of this information product? <input checked="" type="checkbox"/> No <input type="checkbox"/> Yes If so, state these objections. Does this information product contain copyrighted material? <input checked="" type="checkbox"/> No <input type="checkbox"/> Yes If so, identify the page numbers _____ and attach the license or other authority for the government to reproduce.	
8. Submitted by Gleb Mamantov and E. L. Wehry, co-Principal Investigators Organization Department of Chemistry, University of Tennessee, Knoxville, TN 37996	Name and Position (Please print or type)
Signature 	Phone (615) 974-3465
	Date May 9, 1995

FOR DOE OR OTHER AUTHORIZED  
USE ONLY

## 9. Patent Clearance ("x" one)

a. DOE patent clearance has been granted by responsible DOE patent group.  
 b. Report has been sent to responsible DOE patent group for clearance.

## CONTENTS

Introduction.....	2
A. Fractionation of Fly Ash Samples.....	3
B. Phototransformation of Pyrene Sorbed on Fly Ash Fractions.....	9
C. Phototransformation of 1-Nitropyrene Sorbed on Fly Ash Fractions.....	11
D. Measurement of Fractal Dimensions of Coal Fly Ash Particles.....	13
E. Heats of Adsorption of Toluene on Fly Ash Fractions.....	17
F. Effects of Co-Adsorbates on the Phototransformation of Adsorbed PAHs.....	18
G. Identification of Benz[a]anthracene Phototransformation Products.....	20
H. Interactions of Particulate-Phase PAHs with Hydroxyl Radicals.....	21
References Cited.....	21
Publications.....	25
Research Presentations.....	25
Personnel.....	25

## DISCLAIMER

This report was prepared as an account of work sponsored by an agency of the United States Government. Neither the United States Government nor any agency thereof, nor any of their employees, makes any warranty, express or implied, or assumes any legal liability or responsibility for the accuracy, completeness, or usefulness of any information, apparatus, product, or process disclosed, or represents that its use would not infringe privately owned rights. Reference herein to any specific commercial product, process, or service by trade name, trademark, manufacturer, or otherwise does not necessarily constitute or imply its endorsement, recommendation, or favoring by the United States Government or any agency thereof. The views and opinions of authors expressed herein do not necessarily state or reflect those of the United States Government or any agency thereof.

DISTRIBUTION OF THIS DOCUMENT IS UNLIMITED

*W*

MASTER

## **DISCLAIMER**

**Portions of this document may be illegible  
in electronic image products. Images are  
produced from the best available original  
document.**

## INTRODUCTION

The major objective of this work was to characterize the interactions of coal fly ash with polycyclic aromatic hydrocarbons and their derivatives, and to attempt to understand the influence of the surface properties of coal ash (and other atmospheric particles) on the chemical transformations of polycyclic aromatic compounds.

Polycyclic aromatic hydrocarbons (PAHs) and their derivatives are produced in the incomplete combustion of carbonaceous fuels. The compounds are of concern because some of them undergo can undergo metabolic conversion in the body to mutagenic and carcinogenic species [1]. Consequently, the chemical fate of PAHs, under real and simulated environmental conditions, has received considerable attention [2-7].

In the atmosphere, PAHs and their derivatives may occur both in gas and particulate phases. PAHs formed in the vapor phase via combustion processes undergo cooling as they enter the atmosphere; as they are cooled, they may deposit onto particulate matter. While some low-molecular weight PAHs, such as anthracene, phenanthrene, and the benzofluoranthenes, exist in the atmosphere at appreciable equilibrium concentrations in the vapor phase, less volatile compounds (e.g., PAHs containing five or more rings) are encountered primarily in the particulate phase [8-10]. The highest concentrations of organic compounds often are associated with particles in the respirable size range [11]. The atmospheric residence times of these small particles are relatively long (perhaps 4 days or more); hence, organic compounds adsorbed on them may be transported over large distances [12,13].

Subsequent to release into the atmosphere, PAHs and their derivatives may undergo chemical transformation; both photochemical and nonphotochemical processes may take place. Such processes can have important ramifications, especially when the products are more hazardous than the parent compounds (e.g., conversion of PAHs to strongly mutagenic nitro derivatives [14]). The chemical fate of PAHs in the vapor phase has received extensive and careful study, especially by Atkinson and co-workers [7,15,16], and appears to be well understood. However, the nature of chemical transformation of PAHs in the particulate phase, and the manner in which such phenomena may be influenced by the chemical and physical properties of the particulate matter, is much less fully characterized and understood [5].

The chemical fate of a PAH in the particulate phase is known to depend on the physical properties and/or chemical composition of the surface on which it is sorbed. For example, photochemical oxidation of PAHs sorbed on wood soot [17], alumina, silica gel [18,19], glass [A15], and airborne particles sampled via high-volume filtration [21,22] is reported to proceed rapidly, whereas PAHs adsorbed on carbon black [20] and many (but not all) coal fly ashes [18,23-25] are quite resistant to photodecomposition.

Our studies have concentrated on the photochemical behavior of PAHs sorbed from the vapor phase on coal fly ashes, and compositional subfractions obtained therefrom. The PAHs are deposited onto the fly ash substrates from the vapor phase, using apparatus and techniques developed in this laboratory [26,27], in order to simulate, as closely as possible under laboratory conditions, the processes by which PAHs deposit onto fly ash particles in the atmosphere [28].

TABLE I. Mass Distributions of Size Fractions of KA Fly Ash

Size Fraction	Particle Size Range, $\mu\text{m}$	Wt % of Unfractionated Ash
U1	< 45	70
U2	45-74	16
U3	75-124	10
U4	125-149	2
U5	> 150	2

Inasmuch as 70% of the particle mass comprised particles less than 45  $\mu\text{m}$  in diameter, the percentage, on a numerical (rather than mass) basis of < 45  $\mu\text{m}$  particles must have been considerably greater than 70% in the KA ash.

Listed in Table II are the carbon and iron contents (as weight percentages) of the major fractions produced from the "Kaneb" fly ash (hereafter denoted "KA"). Note that the unfractionated ash is relatively high in carbon (both the 45-74 and 75-124  $\mu\text{m}$  size fractions of the unseparated ash are greater than 6 %C).

TABLE II. Carbon and Iron Content of KA Fly Ash Fractions

Fraction and Abbreviation	Particle Size, $\mu\text{m}$	%C	%Fe
Unfractionated (U0)	-	5.5	5.9
Unfractionated (U1)	< 45	2.8	nd
Unfractionated (U2)	45-74	4.7	nd
Carbonaceous (C2)	45-74	23.2	2.0
Mineral (M2)	45-74	0.94	3.1
Magnetic (F2)	45-74	0.56	35.0
Unfractionated (U3)	75-124	7.4	-
Carbonaceous (C3)	75-124	67.3	1.56
Mineral (M3)	75-124	0.87	5.70
Magnetic (F3)	75-124	0.64	46.2

nd : not determined

There is a general trend for the percentage carbon to increase as the particle diameter increases (% C increases in the order U1 < U2 < U3), as noted previously by other investigators [33]. Clearly, the various fractions differ dramatically in composition. Particularly noteworthy are fractions C3 (67.3% C) and F3 (46.2% Fe). The mineral and magnetic fractions (F2, F3, M2, M3) are all less than 1% C, showing that the fractionation technique can be highly effective for separation of the carbonaceous particles from the others.

The specific surface areas, as determined by the classical Brunauer-Emmett-Teller (BET) method using nitrogen adsorption, and colors (determined using Munsell Color Charts [38]) are quite different for the KA ash fractions, as noted in Table III (next page).

TABLE III. Specific Surface Areas and Color Designations of KA Fly Ash Fractions

Fraction and Abbreviation	Surface Area, m <sup>2</sup> /g	Munsell Notation	Color Name
Unfractionated (U0)	3.7	nd	nd
Unfractionated (U2)	5.2	nd	nd
Carbonaceous (C2)	17.2	nd	nd
Magnetic (F2)	0.7	nd	nd
Light mineral (M2A)	1.6	nd	nd
Heavy mineral (M2B)	1.3	nd	nd
Unfractionated (U3)	4.7	5Y 3/1	very dark grey
Carbonaceous (C3)	25.3	N 2/0	black
Magnetic (F3)	1.4	N 3/0	very dark grey
Light Mineral (M3A)	0.9	5YR 5/1	grey
Heavy Mineral (M3B)	0.9	N 4/0	dark grey

nd: not determined

Not surprisingly, the carbonaceous fraction exhibits by far the greatest specific surface area of any of the KA fly ash fractions. (In fact, a plot of the specific surface areas of the various fractions vs. their carbon content in weight percentage forms a very good straight line). A large fraction--at least 80%--of the surface area of the unfractionated ash (U3) can be attributed to the carbonaceous particles, despite the fact that this fraction is only 4.7% C by weight. Therefore, it can be anticipated that the role of the carbonaceous particles in this fly ash (and in many other coal fly ashes) in providing surface sites for adsorption of organic molecules is very much greater than might be inferred from the weight percentage of carbon in the ash. Even if the carbonaceous particles exhibit no greater affinities for organic adsorbates than any of the other particulate phases present in fly ash, just on statistical grounds alone it can be inferred that a sizable fraction of organic adsorbate molecules will be associated with the carbonaceous particles--due solely to their much greater surface areas. In contrast, the extremely low surface area of the magnetic particles indicates that they will play only a minor role in sorption of PAHs unless they have a much greater affinity for PAHs than any of the other particulate phases, which seems highly unlikely.

A second fly ash that we fractionated was produced via combustion of a Texas lignite (hereafter denoted "TX" ash). PAHs sorbed on this ash generally exhibit significant photoreactivity [25]. The mass distributions for the various size fractions of this ash are listed in Table IV.

TABLE IV. Mass Distributions of Size Fractions of TX Fly Ash

Size Fraction	Particle Size Range, $\mu\text{m}$	Wt % of Unfractionated Ash
U1	< 45	48
U2	45-74	20
U3	75-124	24
U4	125-149	4
U5	> 150	4

Comparison of Tables I and IV shows that the TX ash is considerably richer in particles falling within size ranges 2 and 3 (45-74 and 75-124  $\mu\text{m}$ , respectively) than the KA ash. On a numerical basis, particles less than 45  $\mu\text{m}$  in diameter are by far the most numerous in the TX ash, just as in the KA ash.

Chemical composition data for various fractions generated from the TX ash are compiled in Table V. Some fractions analyzed for the KA ash (see Table II) could not be obtained in sufficient quantity from the TX ash to be studied.

TABLE V. -- Carbon and Iron Content of TX Fly Ash Fractions

Fraction and Abbreviation	Size, $\mu\text{m}$	%C 0.84	%Fe 3.4
Unfractionated (U0)	-		
Unfractionated (U1)	< 45	0.50	nd
Unfractionated (U2)	45-74	0.65	nd
Unfractionated (U3)	75-124	0.60	3.4
Carbonaceous (C3)	"	23.0	1.7
Heavy mineral (M3B)	"	0.65	2.4
Magnetic (F3)	"	0.15	36.4
Unfractionated (U4)	125-149	0.63	nd
Unfractionated (U5)	> 150	0.94	nd

nd: not determined

In this relatively low-carbon ash, the trend of increasing carbon content with increasing particle size is not as pronounced as in the higher-carbon KA ash. The carbonaceous fraction of the TX ash, though only 23.0% C by weight, is enriched in carbon by a factor of 40 compared with the unfractionated ash.

Surface areas have been obtained for a variety of fractions produced from the TX ash. These data are compiled in Table VI (next page).

As for the KA ash (Table III), the carbonaceous fractions of the TX ash exhibit significantly larger specific surface areas than any of the other fractions. Interestingly, the surface areas of the mineral fractions (magnetic and non-magnetic) of the TX ash tend to be greater than those of the KA ash. Just as in the KA ash, however, the most significant contributor to the surface area of the unfractionated ash, in any size fraction that we studied, is the carbonaceous fraction. For ash size fraction 3 (i.e., sample U3), more than 50% of the surface area is contributed by the carbonaceous fraction (C3), even though fraction C3 constitutes only about 5% of the total mass of U3.

TABLE VI. Specific Surface Areas of Various TX Fly Ash Fractions

Fraction and Abbreviation	%C	Surface Area, $\text{m}^2/\text{g}$
Unfractionated (U1)	0.50	3.2
Magnetic (F1)	nd	1.9
Heavy Mineral (M1B)	nd	2.7
Unfractionated (U2)	0.65	2.3
Carbonaceous (C2)	12.7	13.1
Heavy Mineral (M2B)	nd	2.7
Unfractionated (U3)	0.60	3.0
Carbonaceous (C3)	23.0	25.6
Heavy Mineral (M3B)	0.65	2.3
Magnetic (F3)	0.15	1.3

nd : not determined

The final example is a stack ash obtained from the University of Tennessee (UT) power plant. This ash (hereafter denoted "UT" ash) was extraordinarily high in carbon content (22.5 %C). The results of the fractionation of this ash are compiled in Table VII. A very large number of fractions was generated from this ash; compositions and surface areas of some of the more significant fractions are compiled in Table VII.

TABLE VII. Carbon and Iron Content, and Surface Area, of UT Fly Ash Fractions

Fraction and Abbreviation	Size, $\mu\text{m}$	%C	%Fe	SA, $\text{m}^2/\text{g}$ <sup>a</sup>
Unfractionated (U0)	-	22.5	nd	nd
Carbonaceous (C1)	< 45	30.4	4.0	14.0
Magnetic (F)	< 45	4.4	37.8	2.9
Carbonaceous (C2)	45-74	65.9	1.7	20.0
Magnetic (F2)	45-74	0.7	39.6	0.5
Carbonaceous (C3)	75-124	72.5	1.8	17.0
Mineral (M3)	75-124	0.5	5.3	0.7
Magnetic (F3)	75-124	0.4	37.6	0.5

<sup>a</sup>specific surface area. nd : not determined.

The wide variety of carbon and iron percentages in the various fractions is especially noteworthy. Also significant is the wide variety of specific surface areas exhibited by these fractions, ranging from 0.5 to 20  $\text{m}^2/\text{g}$ . Not surprisingly, the carbonaceous fractions exhibit much larger specific surface areas than do either the magnetic or mineral fractions. Because of the high carbon content of this ash, it was impossible in some cases to obtain "non-carbonaceous" fractions; for example, the ostensibly magnetic fraction F1 also contains significant numbers of carbonaceous particles, as indicated by its high carbon content (4.4 %C).

We conclude that our fractionation procedure is capable of generating carbonaceous, mineral, and magnetic fractions from a wide variety of heterogeneous fly ash samples.

#### B. PHOTOTRANSFORMATION OF PYRENE SORBED ON FLY ASH FRACTIONS

During the period of this grant, numerous studies of the susceptibility of pyrene, a model 4-ring PAH, to photodecomposition when sorbed on various fly ash fractions were carried out. In these experiments, all samples were prepared by vapor deposition of vapor-phase pyrene onto fly ashes or ash fractions [26,27]. Each sample was illuminated with a xenon lamp whose spectrum is similar to that of sunlight; typically, the area of the sample that was illuminated was 1-3 cm<sup>2</sup>, and the radiant intensity was ca. 0.014 W/cm<sup>2</sup> (considerably greater than that of ambient sunlight). The characteristics of this illumination source are described in detail in the literature [39,40], and the characteristics of our illumination apparatus also are described in detail in the literature [23,41]. Unless stated otherwise, the period of illumination was 24 hours. When illuminated, each pyrene-containing fly ash sample was contained in a quartz cell and a rotary photoreactor design [41] was employed. It has been shown in this and other laboratories that the rotary illumination cell is as effective in ensuring uniform illumination of these solid samples as other, more complex, designs [23,24].

In Table VIII are presented representative data for the extent of photodecomposition of pyrene adsorbed on fractions of the KA ash (cf. Tables I-III for the properties of these fractions).

TABLE VIII. Pyrene Phototransformation on KA Fly Ash Fractions

Fraction and Abbreviation	%C	[Py] <sub>o</sub> , $\mu\text{g/g}$	[Py] <sub>f</sub> , $\mu\text{g/g}$	% Change
Unfractionated (U3)	7.4	96 $\pm$ 5	89 $\pm$ 3	7
Carbonaceous (C3)	67.3	35 $\pm$ 3	34 $\pm$ 4	3
Magnetic (F3)	0.64	25 $\pm$ 3	24 $\pm$ 3	8
Light mineral (M3A)	0.25	41 $\pm$ 4	32 $\pm$ 3	22
Heavy mineral (M3B)	0.78	65 $\pm$ 4	44 $\pm$ 8	32

In Table VIII, [Py]<sub>o</sub> and [Py]<sub>f</sub> are the quantities of extractable pyrene per gram of fly ash before and after illumination, respectively. Clearly, the extent of loss of pyrene was significantly greater for the light and heavy mineral fractions (low both in carbon and iron content--cf. Table II--and a light grey in color) than for the magnetic fraction (low in carbon but high in iron content; dark in color) and the unfractionated ash and carbonaceous fractions (high in carbon content; black in color).

Analogous data are shown in Table IX (next page) for pyrene adsorbed on selected fractions of the Texas lignite (TX) fly ash (see Tables IV-VI for the properties of these fractions).

TABLE IX. Pyrene Phototransformation on TX Fly Ash Fractions

Fraction and Abbreviation	%C	[Py] <sub>0</sub> , $\mu\text{g/g}$	[Py] <sub>f</sub> , $\mu\text{g/g}$	% Change
Unfractionated (U3)	0.60	52 $\pm$ 2	41 $\pm$ 2	21
Carbonaceous (C3)	23.0	105 $\pm$ 2	102 $\pm$ 2	3
Magnetic (F3)	0.15	22 $\pm$ 1	19 $\pm$ 2	15
Heavy Mineral (M3B)	0.65	87 $\pm$ 3	65 $\pm$ 3	26

In contrast with the KA ash, pyrene exhibits significant phototransformation when sorbed on all TX ash fractions except the carbonaceous fraction. Even for the magnetic fraction, which is 36.4% iron, significant pyrene photoreactivity is observed, though pyrene is less photoreactive when sorbed on the magnetic fraction than the unfractionated TX ash or the mineral nonmagnetic fraction. The TX fly ash is much lighter in color than the KA ash; only the carbonaceous fraction is dark in color.

Finally, Table X summarizes studies of the phototransformation of pyrene sorbed on various fractions of the UT ash (see Table VII for compositions and surface areas).

Table X. Pyrene Phototransformation on UT Fly Ash Fractions

Fraction and Abbreviation	%C	[Py] <sub>0</sub> , $\mu\text{g/g}$	[Py] <sub>f</sub> , $\mu\text{g/g}$	% Change
Carbonaceous (C1)	30.4	564	539	4
Magnetic (F1)	4.4	95	92	3
Magnetic (F1)	4.4	16.7	15.8	5
Carbonaceous (C2)	65.9	523	522	0
Carbonaceous (C2)	65.9	107	109	0
Magnetic (F2)	0.7	11.2	6.6	41
Carbonaceous (C3)	72.5	289	280	3
Carbonaceous (C3)	72.5	66	69	0
Mineral (M3)	0.5	17.8	10.0	44
Magnetic (F3)	0.4	11.9	6.9	42

For the UT ash, the fractions fall into two strikingly different populations: those on which less than 5% of the initial quantity of pyrene was destroyed via photodecomposition, and those on which more than 40% of the amount of pyrene initially present was destroyed in a 24-hr illumination. As noted in Table X, the amounts of pyrene initially present differed widely in some of these experiments (because the carbonaceous fractions exhibited a much greater uptake of pyrene from the gas phase than did the mineral or magnetic fractions). However, as seen from the data in Table X, studies using fractions F1, C2, and C3 with different amounts of pyrene initially present showed that changes in the initial quantity of pyrene had minimal influence on the fraction of pyrene initially present that was destroyed.

The only parameter that correlates with the photodecomposition data for the UT ash is the percentage carbon. For any ash fraction that was greater than 1% C by weight, pyrene exhibited negligible photodecomposition. This was true even for

fractions that were nominally "non-carbonaceous". For example, fraction F1 is nominally a magnetic fraction. However, despite strenuous efforts in the fractionation procedure, fraction F1 contained a significant number of carbonaceous particles (4.4% C by weight). On fraction F1, pyrene underwent negligible photodecomposition.

However, for those few fractions of the UT ash that were less than 1% C, significant (> 40%) loss of pyrene upon illumination was noted--specifically, fractions F2, M3, and F3. It should be noted that the iron contents of fractions F2 and F3 were relatively high (39.6 and 37.6% Fe, respectively).

Accordingly, it is difficult to escape the conclusion that the iron content of fly ash samples does not in itself generally influence in a dramatic way the susceptibility of adsorbed pyrene to undergo photodecomposition. However, the presence of significant quantities of carbon (approximately 1 % by weight) in a fly ash or ash fraction is sufficient to suppress virtually totally the tendency of sorbed pyrene to photodecompose.

It is also worth noting that all of the UT ash fractions were black in color (even those that were nominally mineral nonmagnetic fractions). Therefore, the color of a fly ash is not automatically a dominant factor in determining whether a PAH sorbed on that ash will be susceptible to phototransformation. It has previously been surmised that PAH molecules sorbed on very dark fly ash particles may be "shielded" from incident light if they are able to sorb in pores or other surface irregularities [2,23,24,41]. In that situation, one would expect PAHs to resist phototransformation when sorbed on virtually any dark-colored adsorbent (provided that the adsorbent particles had sufficiently irregular surface features to provide opportunities for this "inner-filter effect" [24] to be operative. These issues are addressed further in Section D.

#### C. PHOTOTRANSFORMATION OF 1-NITROPYRENE SORBED ON FLY ASH FRACTIONS

Nitro-substituted polycyclic aromatic hydrocarbons (nitro-PAHs) are believed to be responsible for a portion of the mutagenic activity of organic extracts of atmospheric particulate matter [42]. Many members of this compound class are strong, direct-acting mutagens. Nitro-PAHs are frequently detected in atmospheric particulate matter produced in the combustion of fossil fuels [43]. Some nitro-PAHs, such as 1-nitropyrene and 3-nitrofluoranthene, are thought to be emitted by combustion sources; others (notably 2-nitropyrene and 2-nitrofluoranthene) are believed to be produced by gas-phase atmospheric chemical transformation of the parent PAHs (e.g., via reactions with OH in the presence of NO<sub>2</sub>) [44].

Relatively volatile nitroaromatics, such as the nitronaphthalenes, may exist at appreciable concentrations in the vapor phase in the atmosphere, and may undergo efficient photodecomposition. Less volatile nitro-PAHs, including the nitropyrenes, are expected to be encountered in the atmosphere virtually exclusively in the particulate phase [44]. The susceptibility of particle-associated nitro-PAHs to chemical transformation has been studied much less extensively than that of the parent PAHs. We have accordingly carried out a comparison of the susceptibility to phototransformation of 1-nitropyrene and pyrene, sorbed on the KA fly ash (cf. pp. 4-6) and fractions derived from it. Some comparisons of the photoreactivity of pyrene and 1-nitropyrene were also carried out using silica gel as a model adsorbent.

The weight percentages of carbon and iron for the 45-74  $\mu\text{m}$  size fraction of the KA fly ash and the three subfractions obtained from it are listed in Table XI. These fractions were prepared especially for this study; thus, the compositions in Table XI do not match those for the KA ash fractions compiled in Table II (p. 5). The mineral fraction (M2) accounted for 77% of the mass of the original ash sample; the ferromagnetic fraction (F2) was responsible for 12%, and the carbonaceous fraction (C2) comprised the remaining 11% of the original ash sample (U2).

TABLE XI. Carbon and Iron Content of KA Ash Fractions Used in this Investigation

Fraction and Abbreviation	%C	%Fe
Unfractionated (U2)	6.25	8.2
Magnetic (F2)	<0.5	43.9
Mineral (M2)	0.94	3.3
Carbonaceous (C2)	23.2	4.8

Results of studies of the phototransformation of pyrene and 1-nitropyrene (24 hr illuminations; experimental conditions as described on p. 9) are compiled in Tables XII and XIII, respectively.

TABLE XII. Phototransformation of Pyrene on Silica Gel and KA Fly Ash Fractions

Adsorbent	Initial Conc., $\mu\text{g/g}$	Conc. After Illumination, $\mu\text{g/g}$	Apparent % Loss
Silica Gel	1980	644	68
KA U2	928	839	10
KA F2	153	139	9
KA M2	228	181	21
KA C2	2693	2608	3

TABLE XIII. Phototransformation of 1-Nitropyrene on Silica Gel and KA Ash Fractions

Adsorbent	Initial Conc., $\mu\text{g/g}$	Conc. After Illumination, $\mu\text{g/g}$	Apparent % Loss
Silica Gel	981	577	41
Silica Gel	981	657	33
KA U2	98	98	0
KA U2	52	53	0
KA F2	64	56	12
KA F2	58	52	10
KA M2	85	68	20
KA M2	111	88	21
KA C2	67	71	0
KA C2	67	73	0

Trends in the data compiled in Table XII closely parallel those observed for pyrene sorbed on the KA fly ash and "model" adsorbents (such as silica gel); i.e., pyrene exhibits significant photodecomposition upon 24-hr illumination when sorbed on silica gel and the mineral fly ash fraction, and modest photodecomposition loss when associated with the magnetic fly ash fraction. However, when sorbed on the carbonaceous fly ash fraction, pyrene exhibits virtually no detectable photo-

transformation. The data in Table XIII indicate that the same general trends are observed for 1-nitropyrene.

1-Nitropyrene appears to exhibit a greater affinity for the carbonaceous fly ash particles than does pyrene; in supercritical-fluid extraction studies of the two adsorbates on the C2 fraction of KA fly ash, extraction recoveries were consistently smaller for 1-nitropyrene than for pyrene. Because the sorbed quantities of 1-nitropyrene employed in these experiments represented a very small fraction of a "monolayer" and the unfractionated ash was 11% "carbonaceous particles", and in view of the fact that the carbonaceous particles have much larger specific surface areas than the mineral particles, it is reasonable to presume that, in our experiments with the unfractionated ash (U2), most 1-nitropyrene molecules were associated with the carbonaceous particles.

The KA fly ash contained an atypically high percentage of carbon. The weight percentage of elemental carbon present in actual atmospheric coal fly ash may be lower than that used in this work by more than an order of magnitude [45]. However, the 1-nitropyrene adsorbent coverage levels used in this work are at least two orders of magnitude greater than those typically found for 1-nitropyrene (and other nitro-PAHs) associated with atmospheric particulate matter (reported concentrations usually are 0.6  $\mu\text{g/g}$  or less, even in severely polluted atmospheres [42,43,46]). Accordingly, we infer that photolysis does not generally represent a significant removal mechanism for 1-nitropyrene (or other nitro-PAHs) associated with atmospheric particles except in the special, and unusual, case of particulate matter containing virtually no elemental carbon. This contrasts strongly with the behavior of gas-phase nitro-PAHs, which appear to be quite susceptible to photodecomposition [47].

#### D. MEASUREMENT OF FRACTAL DIMENSIONS OF COAL FLY ASH PARTICLES

PAHs are less susceptible to photochemical transformation when sorbed on coal fly ash than on other types of particulate matter. One plausible explanation of this fact is that fly ash particles (especially carbonaceous particles) are often porous and dark in color. Thus, it is conceivable that sorbed PAH molecules penetrate into pores and thus are "shielded" from incident light [2,23]; cf. also p. 11.

If this picture is valid, coal fly ash surfaces may tend to exhibit fractal properties. A "fractal surface" [48] is a surface in which increased detail is revealed as the surface is viewed at an increasingly high degree of magnification. The extent to which a surface exhibits fractal properties can be regarded as a measure of the "roughness" of that surface. Thus, if sequestration of sorbed PAH molecules in pores with resulting "shielding" of the adsorbate molecules from incident light is really an important phenomenon, one would expect to observe a correlation between the photoreactivity of a PAH sorbed on a surface and the fractal characteristics of that surface.

The degree of "roughness" of a surface is expressed quantitatively in terms of its fractal dimension [49,50]. The numerical value of the fractal dimension ranges from 2.0 (for a perfectly smooth surface) to a maximum value of 3.0. The larger the value of the fractal dimension, the greater the irregularity of the surface. The fractal dimension can (and usually does) have a nonintegral value.

Numerous techniques have been employed to measure fractal dimensions of particulate solids. We have employed two techniques, one based on gas-adsorption measurements, and the other using small-angle X-ray scattering (SAXS) data. The SAXS measurements were carried out at the Oak Ridge National Laboratory, Center for Small-Angle Scattering Research, in collaboration with Dr. J. S. Lin. These methods are based on completely different underlying physical principles. Thus, if the fractal dimensions obtained using these techniques present a self-consistent picture, one has increased confidence that the picture is valid.

In the gas-adsorption technique, different small gaseous molecular adsorbate molecules (e.g., nitrogen, methane, n-propane, n-butane) are used as "rulers" to infer the degree of roughness of a particulate surface. The relative adsorption of the different adsorbates is measured as a function of the adsorbate (gas) pressure at equilibrium with an adsorbent sample, under conditions in which the degree of "surface coverage" of the adsorbent on the adsorbate is greater than a monolayer. As discussed by Avnir and Jaroniec [51], such measurements can yield fractal dimensions for particulate solids without knowing the molecular area of the adsorbate. This is important, because the molecular areas of many adsorbate molecules are not known accurately.

The equation used to process the data is [51]:

$$\theta = N/N_m = K \{ \ln (P_o/P) \}^{D-3} \quad (1)$$

where  $\theta$  is the fractional coverage of the adsorbent surface by the adsorbate,  $N$  is the number of adsorbate molecules adsorbed in a given measurement,  $N_m$  is the number of adsorbed molecules that constitutes a monolayer of the adsorbate,  $P$  is the equilibrium pressure of the adsorbate, and  $P_o$  is the saturation pressure of the adsorbate.  $K$  is a characteristic constant for a particular adsorbent-adsorbate pair, and  $D$  is the fractal dimension (the quantity of interest). From the experimentally measured values of  $N$  as a function of  $P$ , a plot of  $\ln(N/N_m)$  vs.  $\ln(P_o/P)$  is prepared; the slope of the linear portion of the plot for multilayer adsorption (i.e.,  $\ln(N/N_m) > 0$ ) is  $D-3$ . The experimental data are obtained using a commercial surface-area measurement apparatus.

In small-angle X-ray scattering [52], a collimated beam of X-rays impinges upon the sample of interest, and a portion of that beam is elastically scattered. The intensity of the scattered radiation is measured as a function of the scattering angle. X-ray scattering from a structure having a characteristic size  $l$  depends on the product  $ql$ , where

$$q = 4\pi\lambda^{-1} \sin\left(\frac{\theta}{2}\right) \quad (2)$$

The intensity of scattering,  $I(q)$ , from a fractal surface conforms to a power law and is proportional to  $q$  raised to some exponent:

$$I(q) \propto q^{6-D} \quad (3)$$

Two fly ashes have been examined by these techniques: the KA and TX fly ashes, and the fractions derived therefrom, described on pp. 4-7. The KA fly ash is a bituminous coal fly ash that is relatively high in carbon and dark in color. PAHs sorbed on the KA ash undergo virtually no detectable photodecomposition (except on the mineral nonmagnetic fraction; cf. Table VIII). The TX ash is a lignite fly ash that is relatively low in carbon content and light in color. PAHs sorbed on the TX ash are highly photoreactive (except on the carbonaceous fractions; see Table IX).

The fractal dimensions obtained by gas adsorption (GA) and small-angle X-ray scattering (SAXS) are compared in Table XIV (next page).

While the analysis of these data is not yet complete, the following statements can be made:

- (a) All samples exhibit fractal dimensions that fall within the meaningful range (2.00-3.00).
- (b) Many of the fly ashes and ash fractions exhibited relatively large D values (>2.50), suggesting that significant surface "roughness" is a rather common characteristic of these fly ash particles.
- (c) The D values obtained by gas adsorption and SAXS often do not agree. For the KA ash in particular, virtually the same fractal dimension ( $2.67 \pm 0.10$ ) was exhibited by all fractions when gas adsorption data were used to calculate the D values. However, D values obtained by SAXS were much less uniform (ranging from 2.27 to 2.94 for the various KA ash samples that were studied). The relative validities of these two sets of D values is presently not known; this question is currently receiving detailed examination.
- (d) Using the SAXS data for the KA ash, it can be seen that those fractions on which sorbed pyrene exhibited detectable photodecomposition (the various nonmagnetic mineral fractions) appear to have the smallest fractal dimensions (i.e., the "smoother" surfaces). This observation is consistent with the hypothesis that sorbed pyrene (or any other PAH) will be most likely to exhibit detectable photodecomposition when the adsorbent surface is relatively smooth and regular. However, this conclusion must be regarded as tentative; the fractal dimensions measured by gas adsorption show no such trend.
- (e) For the TX ash, the only fractions on which sorbed pyrene is photochemically unreactive (i.e., the carbonaceous fractions) exhibit relatively large fractal dimensions when measured both by both GA and SAXS. However, the D values for those fractions are only slightly larger than those for the other fractions (on which sorbed pyrene exhibits significant photoreactivity).

TABLE XV. Heats of Adsorption of Toluene of "KA Ash" Fractions<sup>a</sup>

Fly Ash Fraction Code	Description of Fraction	%C <sup>b</sup>	Surface <sup>c</sup> Area, m <sup>2</sup> /g	ΔH, kJ/mole
U3	unfractionated ash, 75-124 μm particle size	7.4	nd <sup>d</sup>	38
C2	carbonaceous, 45-74 μm particle size	31.4	13.1	59
C3	carbonaceous, 75-124 μm particle size	67.3	25.6	65
F3	magnetic, 75-124 μm particle size	0.64	0.36	35
M3A	light nonmagnetic mineral, 75-124 μm particle size	nd <sup>d</sup>	1.71	29
M3B	heavy nonmagnetic mineral, 75-124 μm particle size	0.49	1.57	35

<sup>a</sup>Determined for surface coverage of 4 μmoles toluene/g ash.

<sup>b</sup>Weight percentage carbon present in ash.

<sup>c</sup>Specific surface areas determined by BET nitrogen adsorption.

<sup>d</sup>Not determined.

Not surprisingly, the heat of adsorption of toluene is greater for the carbonaceous fractions than for the mineral magnetic or nonmagnetic fractions. For most of the fractions, the measured heat of adsorption decreases as the quantity of toluene injected onto the column is increased. This is the anticipated behavior for any adsorbent that is heterogeneous [54]. For a homogeneous adsorbent (which most fly ashes certainly are not), nearly all adsorption "sites" for a particular solute exhibit virtually the same affinity for that solute; hence, the measured heat of adsorption is virtually independent of the quantity of adsorbate injected (so long as the quantity of adsorbate is less than that required to achieve monolayer coverage of the adsorbent).

#### F. EFFECTS OF CO-ADSORBATES ON THE PHOTOTRANSFORMATION OF ADSORBED PAHs

In both this and other laboratories, studies of the chemical transformation of sorbed organic compounds have generally been carried out using relatively "clean" particulate surfaces containing a single adsorbate. However, real atmospheric particulate matter contains a wide variety of co-adsorbed organic compounds [56]. The nature of the surface sites occupied by any particular adsorbate may be altered by the presence of other adsorbates.

The possibility of "multilayering" also should be considered. When semivolatile organic compounds adsorb on particles, the least volatile compounds presumably condense first, followed by the more volatile compounds. Thus, a relatively volatile compound (such as a 4-ring PAH) may in some instances be "dissolved" in an organic

film, rather than directly "bound" to the particulate surface.

It has been reported that the rates of chemical transformation of polychlorinated dioxins and dibenzofurans sorbed on municipal incinerator fly ash particles may be affected dramatically by other (unknown) organic compounds present as co-adsorbates on the fly ash particles [57]. Such effects have, as yet, not been investigated for PAHs or other semivolatile organics sorbed on coal fly ash. Accordingly, we commenced a study of the effect of long-chain aliphatic hydrocarbon and carboxylic acid co-adsorbates on the efficiency of photochemical transformation of pyrene adsorbed on fly ash fractions. The hydrocarbon and carboxylic acid co-adsorbates are chosen because these species are often detected on the surfaces of sampled airborne particulate matter [56].

We envision two principal ways in which the presence of co-adsorbed organic compounds on fly ash particles can influence the chemical behavior of adsorbed PAHs:

(a) If a co-adsorbate (less volatile than most PAHs) is already present in significant quantity on a fly ash particle when a PAH deposits, from the vapor phase, onto that particle, the PAH would actually be sorbed on (or, in extreme cases, "dissolved in") an organic matrix, rather than the largely inorganic fly ash surface. Since PAHs dissolved in organic solvents tend to exhibit greater chemical (and photochemical) reactivity than PAHs sorbed on "clean" fly ash surfaces, the effect of such a co-adsorbate might be to increase the efficiency with which the PAH undergoes chemical transformation in the atmosphere.

(b) If a co-adsorbate (more volatile than most PAHs) deposits, from the vapor phase, onto a fly ash particle upon which PAHs have already deposited, the effect of the co-adsorbate might be to "shield" the PAH from sunlight and reactive atmospheric species. In that case, the effect of the co-adsorbate presumably would be to decrease the extent to which the PAH undergoes chemical transformation.

According to this (undoubtedly oversimplified) model, a key characteristic of a co-adsorbate is its volatility--i.e., whether the co-adsorbate deposits on an already-deposited layer of sorbed PAH, or the co-adsorbate deposits before the PAH, thus modifying the particulate surface that sorbed PAH molecules "see".

We began to address this issue by using pyrene as the PAH and two co-adsorbates: n-decane (which is considerably more volatile than most PAHs and would therefore be expected to deposit on fly ash particles after PAHs) and succinic acid (less volatile than most PAHs, and thus likely to be adsorbed before, or concomitant with, a PAH). The fly ash was the "Kaneb ash" described above. Preliminary data obtained in these studies are compiled in Tables XVI and XVII.

-----  
TABLE XVI. Photodecomposition<sup>a</sup> of Pyrene in Absence and Presence of Co-adsorbed 1-Decane

Adsorbent	% Loss, no decane	% Loss, decane present
Silica gel	68 %	37 %
KA ash, unfractionated (U2)	10 %	7 %
KA ash, magnetic fraction (F2)	9 %	9 %
KA ash, carbonaceous fraction (C2)	3 %	1 %
KA ash, mineral fraction (M2)	21 %	7 %

<sup>a</sup> 24-hr illuminations (xenon lamp) in all cases. All fly ash samples were the 45-74  $\mu\text{m}$  particle-size fraction.

TABLE XVII. Photodecomposition<sup>a</sup> of Pyrene in Absence and Presence of Co-adsorbed Succinic Acid

Adsorbent	% Loss, no SA	% Loss, SA present
Silica gel	42 %	70 %
KA ash, unfractionated (U2)	2 %	11 %
KA ash, magnetic fraction (F2)	5 %	6 %
KA ash, carbonaceous fraction (C2)	1 %	3 %
KA ash, magnetic fraction (M2)	9 %	15 %

<sup>a</sup>See footnote to Table XVI. SA: succinic acid.

The data in Tables XVI and XVIII are consistent with the hypotheses set forth above. Co-adsorption of pyrene and decane (which is more volatile than pyrene) tends to decrease the extent to which adsorbed pyrene undergoes photodecomposition. In contrast, co-deposition of pyrene and succinic acid (which is less volatile than pyrene) tends to enhance phototransformation of pyrene. These trends are most noticeable when silica gel (upon which adsorbed pyrene is very susceptible to photolysis) is used as the adsorbent.

These conclusions are tentative, for two reasons. First, the relative uncertainties in many of the data cited in Tables XVI and XVII are large, due mainly to the fact that pyrene exhibits only minimal phototransformation on most KA ash fractions. Similar studies, using fractions of a Texas lignite fly ash, which contains much less carbon, and on which pyrene exhibits much higher photoreactivity than on the KA ash, would alleviate this problem. Second, there is evidence that succinic acid undergoes non-photochemical decomposition under the vapor-phase deposition conditions used in these experiments. We have thus decided to repeat the experiments that yielded the data in Table XVII using stearic acid in place of succinic acid. Stearic acid has been shown to be stable under the deposition conditions that we use. Preliminary data for pyrene phototransformation in the presence of stearic acid show the same trends as those found for stearic acid (Table XVII), but more data are needed before these conclusions can be regarded as firm.

#### G. IDENTIFICATION OF BENZ[a]ANTHRACENE PHOTOTRANSFORMATION PRODUCTS

When a PAH undergoes transformation in the atmosphere, it is not safe to assume that transformation to be an environmentally-benign occurrence. Atmospheric transformation products of PAH may in fact be more hazardous than the parent PAHs. A good example is the conversion of PAHs to nitro-PAHs by atmospheric gas-phase chemistry [15]. It is therefore important to establish the identities of the principal PAH transformation products under environmentally-realistic conditions. For many PAHs, the identities of the major products of their phototransformation in the adsorbed state are not known. It is conceivable that final product distributions could be dependent on the nature of the adsorbent surface. Moreover, photoproducts that are stable to further decomposition in gas- or solution-phase systems may undergo further degradation reactions on solid surfaces. (Alternatively, PAH photoproducts that are unstable in gas or solution phases may be stabilized when adsorbed on fly ash.)

A serious difficulty in "product-identification studies" is that the anticipated photoproducts often are not available in sufficient quantity for confirmation of their identities to be made with confidence. Another problem is that, for some PAHs, the phototransformation products may be quite hazardous to work with. We have

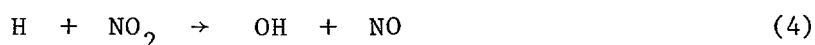
therefore begun our studies with benz[a]anthracene (BaA), for which the principal photoproduct, benz[a]anthracene-7,12-dione, is readily available and not known to be extremely hazardous. As anticipated, we find that the major phototransformation product of BaA, adsorbed both on model adsorbents such as silica gel and on various fractions of the KA and TX fly ashes (see p. 4-6) is benz[a]anthracene-7,12-dione (BaAD). However, BaAD, is itself photosensitive and, upon illumination, undergoes photodecomposition to form products that as yet are unidentified.

The relative photoreactivities of BaA and BaAD depend strongly on the nature of the sorbent surface. For example, on silica gel, the first-order rate constant for phototransformation of BaA is 100 times greater than that for BaAD. However, on a nonmagnetic mineral fraction of the Texas lignite (TX) fly ash, the first-order rate constant for photodecomposition of BaA exceeds that for BaAD only by a factor of 2. (Both compounds exhibit much more rapid phototransformation when sorbed on silica gel than on the lignite ash fraction, but the difference between the photodecomposition rates on the two sorbents is much greater for BaAD than for BaA.) The strong effect of the particulate surface on the relative phototransformation rates of BaA and its oxygenated photoproduct merits additional study.

#### H. INTERACTIONS OF PARTICULATE-PHASE PAHs WITH HYDROXYL RADICALS

In the atmosphere, OH radicals are produced by photochemical reactions involving such species as ozone, hydrogen peroxide, and nitrous acid. Reactions of gas-phase PAHs with OH in the presence of  $\text{NO}_2$  are thought to be a major route for atmospheric production of mutagenic nitro derivatives of PAHs [15]. The question as to whether particulate-phase PAHs are similarly reactive with OH has not been addressed. Accordingly, we attempted to develop apparatus and techniques for performing such investigations.

The apparatus that we assembled for these studies was designed to generate OH radicals by reaction of H atoms with  $\text{NO}_2$ :



The hydrogen atoms were formed via a microwave discharge in a dilute stream of  $\text{H}_2$  and  $\text{NO}_2$  in helium. Detection of hydroxyl radicals was to be achieved via a chemical scavenging ("spin-trap") procedure with identification and quantification of the radical scavenging product by gas chromatography/mass spectrometry, using a published procedure [58].

Despite numerous attempts, and several modifications of the apparatus and analytical procedure, conclusive evidence for production of OH in useful concentrations by this approach was not obtained. Effort in this area of work therefore was suspended. These studies may be resumed in the future, using photolytic generation of hydroxyl radicals [59].

#### References Cited

- [1] H. V. Gelboin and P. O. P. Ts'o, "Polycyclic Hydrocarbons and Cancer", Academic Press, New York (1978).
- [2] T. Nielsen, T. Ramdahl, and A. Bjorseth, Environ. Health Perspect., 47, 103 (1983).

Publications

1. E. L. Wehry and G. Mamantov, Sorption and Photochemical Transformation of Polycyclic Aromatic Hydrocarbons on Coal Stack Ash Particles, in "Aquatic and Surface Photochemistry" (G. Helz, R. Zepp, and D. Crosby, Ed.), CRC Press, Boca Raton, FL, pp. 173-180 (1994).
2. P. S. Holder, E. L. Wehry, and G. Mamantov, Photochemical Transformation of 1-Nitropyrene Sorbed on Coal Stack Ash Fractions, Polycycl. Arom. Cmpds., 4, 135-139 (1994).

[Additional publications ultimately will result from this work; they have not yet been submitted.]

Research Presentations

1. E. L. Wehry and G. Mamantov, Sorption and Transformation of Polycyclic Aromatic Compounds on Coal Stack Ash Particles, paper presented at 203rd national meeting, American Chemical Society, San Francisco, CA, 04/08/92.
2. J. D. Jenkins, E. L. Wehry, and G. Mamantov, Determination of Surface Fractal Dimensions of Coal Fly Ash Subfractions, paper presented at Pittsburgh Conference on Analytical Chemistry and Applied Spectroscopy, Atlanta, GA, 03/11/93.
3. E. L. Wehry and G. Mamantov, Determination of Surface Fractal Dimensions of Coal Fly Ash Subfractions, oral presentation at UCR Contractors' Review Conference, Pittsburgh, PA, 06/25/93.
4. P. S. Holder, J. D. Jenkins, G. M. Woody, G. Mamantov, and E. L. Wehry, Sorption and Chemical Transformation of Polycyclic Aromatic Compounds on Coal Stack Ash Particles, paper presented at 206th National Meeting, American Chemical Society, Chicago, IL, 08/23/93.

PersonnelA. Graduate Students

1. Paul S. Holder, 1991-93 (received Ph.D., December 1993. Now at Southern Testing and Research Laboratories, Wilson, NC)
2. J. David Jenkins, 1991-present (has completed all experimental work and is now writing Ph.D. Dissertation. Now at Salisbury State College, Salisbury, MD)
3. Gary M. Woody, 1991-93 (terminated graduate study without receiving degree)
4. M. Sabella Bowers, 1994-95 (current student; Ph.D. candidate)
5. Kristi C. Anderson, 1994-95 (current student; M.S. candidate)

B. Postdoctoral Research Associate

1. T. Jon D. Dunstan, 1992-94

C. Undergraduate Students

1. Richard P. Holroyd, summer 1993 [Permanent Address: Nottingham Trent University, Nottingham, U.K.]
2. Erika D. Watson, summer 1994 [Permanent Address: Wofford College, Columbia, SC]

Personnel (continued)D. Research Participants (Faculty at Four-Year Colleges)\*

1. David A. Franz, summer 1992 [Permanent Address: Department of Chemistry, Lycoming College, Williamsport, PA]
2. Narendra P. Singh, summer 1993 [Permanent Address: Department of Chemistry, Methodist College, Fayetteville, NC]
3. Todd J. Trout, summer 1994 [Permanent Address: Department of Chemistry, Mercyhurst College, Erie, PA]

\*This program is supported by the National Science Foundation. The indicated individuals participated in the research described in this report.

United States Government

Department of Energy

Pittsburgh Energy Technology Center

# memorandum

DATE: May 17, 1995

REPLY TO  
ATTN OF: Document Control Center, MS 921-143

SUBJECT: Review of Technical/Topical Report on Contract/Grant/  
Cooperative Agreement No. DE-FG22-91PC91306 with  
University of Tennessee

TO: Jerry Harness, Contracting Officer Representative

Scott Penninger (304-285-4790)

The attached technical/topical report has been submitted by  
the contractor/recipient and requires your review and  
approval. Review should be completed within 15 calendar  
days of the date of this memo.

Please provide the contractor/recipient with approval or  
with notification of changes required prior to approval, and  
obtain and approve these changes. A copy of your  
correspondence concerning the report should be provided to  
the Contract Specialist. Your approval shall be indicated  
below and provided to the Document Control Center.

Technical Report for period ending: 03/31/1995



The report has been approved.



The report must be revised.



Attached is a copy of my comments that were  
provided to the contractor/recipient.



Comments: The comments were made on the  
draft report & submitted to the contractor

  
Contracting Officer Representative

6/5/95  
Date

bcc:

Cynthia Mitchell  
DE-FG22-91PC91306  
Document Control  
Letter File

RECEIVED  
95 JUN - 9 AM 10:44  
ACQUISITION & ASSISTANCE  
USDOE/PETC